LIMIT-CYCLE OSCILLATIONS OF AN AIRFOIL WITH PIECE-WISE LINEAR RESTORING FORCES

B.H.K. Lee, L. Liu
ben.lee@nrc.ca , liping.liu@nrc.ca
Aerodynamics Laboratory
National Research Council, Ottawa, Ontario, Canada

Y.S. Wong
Department of Mathematical and Statistical Sciences
University of Alberta, Edmonton, Alberta, Canada
yaushu.wong@ualberta.ca

Keywords: *Nonlinear aeroelasticity, limit-cycle oscillations, piece-wise linear forces, numerical schemes, describing function, point transformation theory.*

Abstract

Nonlinear airfoil motion for incompressible airflow with a piece-wise linear restoring spring force is investigated. It is possible to obtain stable, divergent, limit-cycle oscillations and chaotic motions depending on airfoil parameters and initial conditions. Two numerical time-marching schemes are described and the accuracy is examined. A new method based on a point transformation theory to handle piece-wise linear functions in nonlinear aeroelastic problems is outlined. The results from this technique are used to assess the accuracy and limitations of the numerical schemes and the describing function technique.

1 Introduction

Classical theories in aeroelasticity are based on linear aerodynamics and structures, and they have been used successfully for many decades to predict flutter boundaries and dynamic responses of aircraft to gusts, turbulence and external excitations. Aerodynamics nonlinearities are often encountered at transonic speeds or at high angles of attack where flow separation occurs. Structural nonlinearities arise from worn hinges of control surfaces, loose control linkages, material behaviour and other sources. A comprehensive review on this subject has been reported recently by Lee et al. [1].

Limit-cycle oscillations (LCOs) arising from a concentrated structural nonlinearity in the restoring forces were first studied by Woolston et al. [2] and Shen [3] in the late 1950s. The three basic nonlinearities, namely, cubic, freeplay and hysteresis were investigated using an analog computer [2] and by approximate methods [3]. The cubic case has further been studied in detail by numerical techniques [4], and most recently by an analytical approach [5] using the center manifold theory and the principle of normal form. For piece-wise linear restoring forces, such as the freeplay and hysteresis, an exact analytical solution is only possible with the latest development of a point transformation method [6].

In this paper, various methods of solving nonlinear aeroelastic response of a two-degree-of-freedom airfoil motion with a piece-wise linear restoring force are discussed. The errors in numerical schemes are shown to give inconsistent results in some special cases, and the advantages of using an analytical method that captures the switching points of a piece-wise linear force are demonstrated.

2 Aeroelastic Equations for An Airfoil

Fig. 1 gives the symbols used in the analysis of a two-degree-of-freedom airfoil motion. The plunge deflection is denoted by h, positive in the downward direction, and α is the pitch angle about the elastic axis, positive nose up. The elastic axis is located at a distance $a_h b$ from the midchord, while the mass centre is located at a distance $x_\alpha b$ from the elastic axis, where b is the airfoil semi-chord. Both distances are positive when measured towards the trailing edge of the airfoil. The aeroelastic equations of motion for linear springs have been derived by Fung [7]. For nonlinear restoring forces, the coupled bending-torsion equations for the airfoil can be written as follows:

$$m\ddot{h} + S\ddot{\alpha} + C_h\dot{h} + \overline{G}(h) = p(t), \qquad (1)$$

$$S\ddot{h} + I_\alpha\ddot{\alpha} + C_\alpha\dot{\alpha} + \overline{M}(\alpha) = r(t), \qquad (2)$$

where the symbols m, S, C_h, I_α and C_α are the airfoil mass, airfoil static moment about the elastic axis, damping coefficient in plunge, wing mass moment of inertia about elastic axis, and torsion damping coefficient respectively. $\overline{G}(h)$ and $\overline{M}(\alpha)$ are the nonlinear plunge and pitch stiffness terms, and $p(t)$ and $r(t)$ are the forces and moments acting on the airfoil, respectively.

Defining $\xi = h/b$, $K_\xi = K_h$, $x_\alpha = S/bm$, $\omega_\xi = (K_\xi/m)^{1/2}$, $\omega_\alpha = (K_\alpha/I_\alpha)^{1/2}$, $r_\alpha = (I_\alpha/mb^2)^{1/2}$, $\zeta_\xi = C_h/2(mK_h)^{1/2}$ and $\zeta_\alpha = C_\alpha/2(I_\alpha K_\alpha)^{1/2}$, Eqs. (1) and (2) can be written in nondimensional form as follows [8]:

$$\xi'' + x_\alpha\alpha'' + 2\zeta_\xi\frac{\overline{\omega}}{U^*}\xi' + \left(\frac{\overline{\omega}}{U^*}\right)^2 G(\xi) = -\frac{1}{\pi\mu}C_L(\tau) + \frac{P(\tau)b}{mU^2}, \qquad (3)$$

$$\frac{x_\alpha}{r_\alpha^2}\xi'' + \alpha'' + 2\frac{\zeta_\alpha}{U^*}\alpha' + \frac{1}{U^{*2}}M(\alpha) = \frac{2}{\pi\mu r_\alpha^2}C_M(\tau) + \frac{Q(\tau)}{mU^2 r_\alpha^2}, \qquad (4)$$

where $G(\xi) = \overline{G}(h)/K_\xi$ and $M(\alpha) = \overline{M}(\alpha)/K_\alpha$.

In Eqs. (3) and (4), U^* is a nondimensional velocity defined as $U^* = \frac{U}{b\omega_\alpha}$ and $\overline{\omega} = \frac{\omega_\xi}{\omega_\alpha}$, where ω_ξ and ω_α are the uncoupled plunging and pitching modes natural frequencies, respectively, U is the freestream velocity, and the $'$ denotes differentiation with respect to the nondimensional time τ defined as $\tau = \frac{Ut}{b}$. $C_L(\tau)$ and $C_M(\tau)$ are the lift and pitching moment coefficients, respectively and μ is the airfoil/air mass ratio $(m/\pi\rho^2)$. For incompressible flow, Fung [7] gives the following expressions for $C_L(\tau)$ and $C_M(\tau)$:

$$C_L(\tau) = \pi(\xi'' - a_h\alpha'' + \alpha') + 2\pi\left\{\alpha(0) + \xi'(0) + \left[\frac{1}{2} - a_h\right]\alpha'(0)\right\}\phi(\tau) + 2\pi\int_0^\tau \phi(\tau-\sigma)\left[\alpha'(\sigma) + \xi''(\sigma) + \left(\frac{1}{2} - a_h\right)\alpha''(\sigma)\right]d\sigma \qquad (5)$$

$$C_M(\tau) = \pi(\frac{1}{2} + a_h)\{\alpha(0) + \xi'(0) + (\frac{1}{2} - a_h)\alpha'(\tau)\}\phi(\tau) + \pi(\frac{1}{2} + a_h)\int_0^\tau \phi(\tau-\sigma)\{\alpha'(\sigma) + \xi''(\sigma) + (\frac{1}{2} - a_h)\alpha''(\sigma)\}d\sigma + \frac{\pi}{2}a_h(\xi'' - a_h\alpha'') - (\frac{1}{2} - a_h)\frac{\pi}{2}\alpha' - \frac{\pi}{16}\alpha'' \qquad (6)$$

where the Wagner function $\phi(\tau)$ is given by

$$\phi(\tau) = 1 - \psi_1 e^{-\varepsilon_1\tau} - \psi_2 e^{-\varepsilon_2\tau}, \qquad (7)$$

and the constants $\psi_1 = 0.165$, $\psi_2 = 0.335$, $\varepsilon_1 = 0.0455$ and $\varepsilon_2 = 0.3$ are obtained from Jones [9]. $P(\tau)$ and $Q(\tau)$ are the externally applied forces and moments, respectively, and they are set to zero in this study.

Due to the presence of the integral terms in the integro-differential equations given in Eqs.(3) and (4), it is cumbersome to integrate them numerically. A set of simpler equations was derived by Lee et al. [10], and they introduced four new variables

$$w_1 = \int_0^\tau e^{-\varepsilon_1(\tau-\sigma)}\alpha(\sigma)d\sigma,$$

$$w_2 = \int_0^\tau e^{-\varepsilon_2(\tau-\sigma)}\alpha(\sigma)d\sigma,$$

$$w_3 = \int_0^\tau e^{-\varepsilon_1(\tau-\sigma)}\xi(\sigma)d\sigma, \quad (8)$$

$$w_4 = \int_0^\tau e^{-\varepsilon_2(\tau-\sigma)}\xi(\sigma)d\sigma.$$

The resulting set of eight first-order ordinary differential equations by a suitable transformation is given as follows:

$$d\mathbf{X}/d\tau = \boldsymbol{f}(\mathbf{X},\tau), \quad (9)$$

where $\mathbf{X} = \{x_1, x_2, ..., x_8\} = \{\alpha,\ \alpha',\ \xi,\ \xi',\ w_1,\ w_2,\ w_3,\ w_4\} \in \mathbf{R}^8$.

In this paper, we shall consider a piece-wise linear restoring force represented by a nonlinear freeplay spring in the pitch degree of freedom shown in Fig. 2. The restoring moment is given by the following:

$$M(\alpha) = \begin{cases} M_0 + \alpha - \alpha_f, & \alpha \in (-\infty, \alpha_f) \\ M_0 + M_f(\alpha - \alpha_f), & \alpha \in (\alpha_f, \alpha_f + \delta) \\ M_0 + \alpha - \alpha_f + \delta(M_f - 1), & \alpha \in (\alpha_f + \delta, +\infty) \end{cases} \quad (10)$$

Similar expressions for $G(\xi)$ in the plunge degree-of-freedom can be written with α replaced by ξ.

3 Numerical Solutions

For unforced oscillations, Eqs. (3) and (4) were solved by Lee and Desrochers [8] using Houbolt's [11] finite difference scheme. This method has been shown to be more efficient than higher order finite difference schemes [12] with comparable accuracy. The derivatives at time $\tau + \Delta\tau$ are replaced by backward difference formulas using values at three previous times. In difference form, Eqs. (3) and (4) can be expressed, after considerable algebra [8], as

$$\overline{P}_{11}\alpha(\tau+\Delta\tau) + \overline{P}_{12}\xi(\tau+\Delta\tau) = \overline{X}_1 + T_\xi(\xi), \quad (11)$$

$$\overline{P}_{21}\alpha(\tau+\Delta\tau) + \overline{P}_{22}\xi(\tau+\Delta\tau) = \overline{X}_2 + T_\alpha(\alpha) \quad (12)$$

where $\overline{P}_{11}$, … $\overline{P}_{22}$, $\overline{X}_1$ and $\overline{X}_2$ are coefficients depending on the airfoil parameters and the constants in the Wagner's function. $T_\alpha(\alpha)$ and $T_\xi(\xi)$ contain functions of the nonlinear structures. These are long algebraic terms and are given in Lee and Desrochers [8] for a freeplay nonlinearity. As shown in Eqs. (5) and (6), the aerodynamic forces and moments depend on two integrals. These integrals have to be evaluated at each time step, and in order to reduce the amount of computations, Lee and Desrochers [8] derived a recurrence formula using Simpson's rule. Houbolt's finite difference scheme requires values of α and ξ at times $\tau - 2\Delta\tau$, $\tau - \Delta\tau$ and τ in order to determine the respective values at $\tau + \Delta\tau$. Hence, at time $\tau = 0$, a starting procedure is required and a Talyor's series procedure can be used. The only conditions required to start the numerical scheme are $\alpha(0)$, $\alpha'(0)$, $\xi(0)$ and $\xi'(0)$. The accuracy of Houbolt's scheme is $O(\Delta\tau^4)$ at each time step while the estimations of the starting point limit the accuracy to $O(\Delta\tau^3)$. The global accuracy of the scheme is thus $O(\Delta\tau^3)$.

For the alternative aeroelastic equations given by Eq. (9), a fourth-order Runge-Kutta scheme is commonly used to integrate the system of equations for given initial conditions. Replacing the differentials $d\mathbf{X}$ and $d\tau$ by finite increments $\Delta\mathbf{X}$ and $\Delta\tau$, Eq. (9) becomes

$$\Delta\mathbf{X} = \boldsymbol{f}(\mathbf{X},\tau)\Delta\tau. \quad (13)$$

Denoting $\mathbf{X}^{(n)}$ and $\mathbf{X}^{(n+1)}$ as 8-component vectors at time steps n and n+1, we can write

$$\mathbf{X}^{(n+1)} = \mathbf{X}^{(n)} + \Delta\mathbf{X}. \quad (14)$$

To implement the Runge-Kutta method, the right hand side of Eq. (9) is evaluated four

times for each time step $\Delta\tau$: once at the initial point, twice at trial midpoints, and once at a trial endpoint. From the definitions of w_1 to w_4 given in Eq. (8), the initial values of w_1 to w_4 are equal to zero. The initial conditions of the system can be expressed as

$$\begin{aligned}\mathbf{X}(0) = \mathbf{X}^{(0)} &= [x_1(0), x_2(0), ..., x_8(0)]^T \\ &= [\alpha(0), \alpha'(0), \xi(0), \xi'(0), 0, 0, 0, 0]^T\end{aligned}, \quad (15)$$

where $\alpha(0)$, $\alpha'(0)$, $\xi(0)$ and $\xi'(0)$ are the initial values of pitch displacement, pitch velocity, plunge displacement and plunge velocity respectively.

The Runge-Kutta method is an explicit and stable numerical procedure, and the only input parameter required is the time step $\Delta\tau$. Although the dimension is higher than Houbolt's scheme, there is no need to estimate the starting point. The accuracy of the scheme at each time step is $O(\Delta\tau^5)$, while the global accuracy is $O(\Delta\tau^4)$.

In order to compare the accuracy of Houbolt's and the Runge-Kutta schemes, an example is considered with the following set of parameters:

$$\begin{aligned}&\overline{\omega} = 0.2,\ \mu = 100,\ x_a = 0.25,\ r_\alpha = 0.5,\\ &a_h = -0.5,\ \zeta_\alpha = \zeta_\xi = 0, \alpha_f = 0.25^o, \\ &M_0 = 0.25^o,\ \delta = 0.5^o,\ M_f = 0.\end{aligned} \quad (16)$$

We consider first the results obtained from Houbolt's scheme where $\Delta\tau$ is taken to be 1/128 of the shorter period of the two coupled modes of oscillation of the airfoil in the absence of aerodynamic forces [12], i.e. $\Delta\tau$ is approximately 0.75.

Fig. 3 shows the flutter boundary obtained for the above airfoil parameters. To determine the flutter boundary, Eqs. (11) and (12) are solved for given initial conditions. In this paper only the initial pitch displacement $\alpha(0)$ is varied while $\alpha'(0)$, $\xi(0)$ and $\xi'(0)$ are set to zero. The linear flutter speed U_L^* is first determined from solving the problem for $M_0 = \delta = \alpha_f = 0$. In the nonlinear case, once $\alpha(0)$ is specified, a value of U^* is selected and α and ξ are obtained by the time-marching finite difference scheme. The solution is divergent for $U^* > U_L^*$, and the nonlinear divergent flutter speed is the same as U_L^*. For $\alpha(0) > M_0$, decreasing U^* below U_L^* results in limit-cycle flutter. The range of $\alpha(0)$ is from -10° to 20° in Fig. 3, and it is important to ensure that the steady state pitch and plunge amplitudes are small enough for linear aerodynamics to be applicable.

As U^* decreases away from U_L^*, a value will be reached where any further decrease will result in damped oscillations of the airfoil. Boundaries can be identified in the $\alpha(0)$ versus U^*/U_L^* plots separating the regions of limit-cycle flutter from the stable regions where the airfoil motion decays from the initial displacement to its equilibrium position after the transients die out. In the damped oscillation region, there are pockets where the airfoil oscillates with constant amplitude. These LCO regions [8] are determined using a binary search complemented with linear grid scans. This by no means assures that all such regions, especially the small ones are found. The boundaries are only approximate and depend on the grid used in the searching routine, which in this case is rather coarse.

In the Runge-Kutta scheme, the time step used is the same as that used in Houbolt's scheme, that is, $\Delta\tau$ =0.75. Sufficiently far from the boundary of an LCO pocket, the numerical solutions using these two methods are practically identical. However, there are some cases close to an LCO boundary where these two methods can lead to different numerical solutions. Fig. 4 shows the results from Houbolt's scheme for $\alpha(0) = 8^o$ and $U^*/U_L^* = 0.78$ where a limit-cycle motion is detected. The Runge-Kutta method gives a decaying or stable motion as shown in Fig. 5. This shows that the numerical solutions from the two numerical methods can have different asymptotic behavior.

It is well known that numerical schemes for oscillatory motion of mechanical systems can suffer from two major defects [13, 14],

namely, a period elongation and an amplitude decrement which are functions of the time step. In many applications, the errors introduced can be minimized by choosing a sufficiently small time step. However, accurate prediction of neural stability boundaries numerically can be in error when an artificial damping inherent in the numerical scheme is present. The errors introduced in these two methods are different and hence the numerically determined stability boundary may not coincide exactly.

4 Point Transformation Method

The Houbolt's and Runge-Kutta schemes for solving Eqs. (3) and (4) have an additional drawback when dealing with piece-wise linear functions. On examining Fig. 2, we see that in time-marching schemes, the end points of the middle segment in the restoring force versus displacement plot will not be determined exactly each time the airfoil traverses R_2. This is due to the usual procedure of choosing a uniform time step, and the numerical procedure becomes much more complex if the exact location of the two end points is required. Often, by using a small time step, the error can be controlled to an acceptable level provided that the solution is stable in the sense that a small error in the location of the end points will not give completely different motion behaviour. In Liu et at. [6] a new technique based on the point transformation theory is introduced to deal specifically with piecewise continuous functions.

Consider the eight dimensional system given in Eq.(9) for a freeplay in pitch and a linear spring in plunge. $M(\alpha)$ is given in Eq. (10) and $G(\xi) = \beta\xi$, where β is a constant. In the three linear branches of $M(\alpha)$ shown in Fig. 2, the eight dimensional state space $\mathbf{R}^8$ is divided into three regions, R_i $(i = 1,2,3)$, each of which corresponds to a linear sub-system:

$$\begin{aligned} R_1 &= \{x_1 \in (-\infty, \alpha_f)\} \qquad \mathbf{X}' = A\mathbf{X} + F_1 \\ R_2 &= \{x_1 \in (\alpha_f, \alpha_f + \delta)\} \quad \mathbf{X}' = B\mathbf{X} + F_2 \\ R_3 &= \{x_1 \in (\alpha_f, +\infty)\} \qquad \mathbf{X}' = A\mathbf{X} + F_3 \end{aligned} \tag{17}$$

Here A and B are 8×8 constant matrices, and F_1, F_2 and F_3 are 8×1 constant vectors. The elements of A, B and $F_i (i = 1,2,3)$, determined by the system parameters, are given in Liu et al. [6]. The regions, R_i $(i = 1,2,3)$, and a general phase path of x_2 versus x_1 are shown in Fig. 6. Assuming the motion initially starts at a point X_0, the path begins in R_1 and passes through R_2 into R_3. Then it returns through R_2 back into R_1. Let X_1 and X_2 be the points through which the path enters R_2 and R_3, respectively, and let X_3 and X_4 be the points through which the path leaves R_3 and R_2, respectively. These points (X_1, X_2, X_3 and X_4) are called switching points since they give the locations where the linear subsystems change. We denote the traveling time of the path (from X_1 to X_2) in region R_2 to be t_1, and t_2, t_3 and t_4 be the traveling times of the path in regions R_3, R_2 and R_1, respectively. The above process of the point transformation (X_1 is transformed into X_2, which is then transformed into X_3, and X_3 is transformed into X_4, which is then transformed into X_1^1) then repeats. Two formulations are developed to determine the traveling times and switching points for a nonlinear aeroelastic system with a freeplay.

In the first formulation [6], starting with a given set of initial conditions at X_o, the traveling times are first determined by solving a nonlinear equation, and the switching points are then calculated by multiplying a known matrix with a known vector. Although the method starts with a given set of initial conditions, it is not a time-integration scheme since the solution to each linear subsystem is determined analytically. This formulation is capable of detecting any type of steady state motion including stable, divergent, LCOs and chaotic motions.

The second formulation determines the traveling times and the switching points of an LCO directly without going through the transient state. Only the steady state behavior is considered since no information with respect to the transients is used. This procedure is very efficient if only the steady state solution is of interest, and involves solving a system of

nonlinear algebraic equations. The present formulation can only be used to detect period-one limit-cycle oscillations but can be modified to detect period-*n* LCOs and period-*n* LCOs with harmonics.

Using the airfoil parameters given in Eq. (16), we compute a case corresponding to initial condition $\alpha(0) = 9^o$ at $U^*/U_L^* = 0.78$ using the Runge-Kutta scheme with different time steps. For small time steps up to $\Delta\tau = 0.32$ ($\Delta\tau/T \approx 0.0035$), the motion is periodic with the period $T = 92.45$. As the time step increases by 0.01 to $\Delta\tau = 0.33$ ($\Delta\tau/T \approx 0.0036$), the motion becomes stable rather than periodic. Increasing $\Delta\tau$ to 0.34 ($\Delta\tau/T \approx 0.0037$), the motion changes back to be periodic. Further increasing the time step $\Delta\tau$, the numerical motion keeps changing between a stable motion and a periodic motion. This is a peculiar case that shows the motion to be dependent on $\Delta\tau$ and we suspect that the switching points have a significant effect on the motion. Hence, they must be located accurately in the numerical scheme.

The two formulations of the PT method are applied to this case. The first formulation takes into account the initial conditions and detects four switching points and four traveling times for the steady state motion. The time history for the pitch angle is very similar to that from the Runge-Kutta method with $\Delta\tau \le 0.32$. Using the second formulation gives the same four switching points and four traveling times (t_1 = 10.07, t_2 = 20.2 t_3 = 4.72 and t_4 = 57.45), confirming a periodic motion. The phase path of the pitch angle, the four switching points X_i $(i = 1,2,3,4)$ and the four traveling times t_i $(i = 1,2,3,4)$ for the steady state are displayed in Fig. 7. In cases like this when different time steps in a numerical scheme yield different results, the point transformation method offers distinct advantage over numerical schemes since the solution is analytic and independent of the time step.

5 Describing Function Method

The describing function technique, sometimes referred to as the harmonic balance method, is a method of obtaining an equivalent linear system such that traditional linear aeroelastic methods of analysis can be employed. This method is essentially the same as the first approximation of Kryloff and Bogoliuboff [15].

For a freeplay, *M(α)* is given by Eq. (10) and the airfoil motion is assumed to be of the form:

$$\alpha(\tau) = B + A\sin\omega\tau \ , \qquad (18)$$

where A and B are constants. A dual-input describing function is employed and is given by

$$N = N_B + N_A \sin\omega\tau + N_C \cos\omega\tau \ . \qquad (19)$$

In the above equation, N_A, N_B and N_C are given by [16]

$$N_A = \frac{1}{\pi}\int_{-\pi}^{\pi} M(\alpha)\sin\omega\tau \ d(\omega\tau) = A\left[1 + (1 - M_f)(f(\gamma) - f(\beta))\right]$$

$$N_B = \frac{1}{2\pi}\int_{-\pi}^{\pi} M(\alpha)\, d(\omega\tau) = A[(M_0 + M_f\delta/2)/A - (\gamma+\beta)/2 - (1 - M_f)(g(\gamma) - g(\beta)] \qquad (20)$$

$$N_C = \frac{1}{\pi}\int_{-\pi}^{\pi} M(\alpha)\cos\omega\tau \ d(\omega\tau) = 0$$

where

$$f(x) = \begin{cases} 1/\pi\left(\sin^{-1}x + x(1-x^2)^{1/2}\right), & |x| < 1 \\ -1/2, & x \le -1 \\ 1/2, & x \ge 1 \end{cases} \qquad (21)$$

$$g(x) = \begin{cases} 1/\pi\left(x\sin^{-1}x + (1-x^2)^{1/2}\right), & |x| \le 1 \\ |x|/2, & |x| > 1 \end{cases}$$

$\gamma = (\alpha_f - B)/A$ and $\beta = (\alpha_f + \delta - B)/A$. In Eq. (4) the nonlinear term *M(α)* is replaced by the describing function given in Eq.(19).

However, the describing function depends on the amplitude of oscillation A and B, and thus, an iterative approach is required. First, it should be realized that there is no steady external moment, aerodynamic or otherwise, acting on the airfoil, hence, there can be no steady component to the restoring moment, or N_B must be equal to zero. In the iterative procedure, a value of A is initially assumed, then by setting $N_B = 0$ the value of B is obtained, and so the equivalent linear stiffness given by the describing function is now known. From this point on the equations are solved using standard linear aeroelastic technique. In our case, the U-g method [7] is employed to determine the required value of U^* to give simple harmonic motion. The above procedure is repeated for different values of A, and the variation of A and B with U^* is then obtained.

The describing function method is used to solve the aeroelastic system given by Eq. (16) with M_f = 0.05 /rad. Fig. 8 shows the results of the pitch amplitude plotted against U^*/U_L^* obtained from the describing function method and Houbolt's scheme for $\alpha(0) = -1.0^o$, $\alpha'(0) = \xi(0) = \xi'(0) = 0$. In this figure, the solid line denotes the results from the describing function method, and the filled circles are from the Houbolt's scheme. The describing function solution gives two values of A (A_1 and A_2) for each value of U^*/U_L^*; furthermore, because there is a preload in this case, B is nonzero. In Fig. 8, the values of $B+A_1$ and $B+A_2$ are given. The larger value of the pitch amplitude represents a stable LCO, while the smaller value represents an unstable LCO. For the simple period-one motion the describing function method gives excellent agreement with the Houbolt's scheme. Two cases are studied to compare the describing function with the point transformation method. For $U^*/U_L^* = 0.9$, the result from the point transformation method gives a simple period-one motion as shown in Fig. 9. The airfoil does not oscillate about the zero mean position, indicating that the representation used in Eq. (18) is correct. The time history of the pitch angle determined from the point transformation method gives a periodic solution with maximum amplitude of 1.99^o, which agrees with the describing function prediction of 2^o. When the velocity ratio decreases to $U^*/U_L^* \le 0.83$, the prediction from the describing function does not agree with the result from the point transformation method. For example at $U^*/U_L^* = 0.79$, the time history of the pitch angle resulting from the point transformation method is shown in Fig. 10, while the describing function technique gives a time series similar to Fig. 9. The maximum amplitude of the pitch angle is 1.27° from the point transformation method and it is very close to the result from Houbolt's scheme which gives an amplitude of 1.28°, while the prediction from the describing function method is 1°. We note from this figure that a harmonic is present and the amplitude of the smaller peak in Fig. 10 is approximately 0.2° from both the point transformation and Houbolt's methods. Because the describing function in Eq. (18) assumes a period-one motion, it is not capable of predicting higher order LCOs. The analysis discussed in Johnson [17] can be adopted when higher order harmonics are present, but the analysis involves considerable amount of algebra. This method has not been applied to aeroelastic problems and further studies are required to assess its usefulness. However, at best it can be used to determine LCOs, and unlike the point transformation method, will not be able to predict stable, divergent or chaotic motions.

6 Concluding Remarks

In dealing with piece-wise linear functions, such as a freeplay, the exact location of the switching points where linear segments meet is important in predicting the airfoil motion. These points are usually not located exactly in time-marching numerical schemes using a fixed time step. However, if the motion is not unstable in the sense that a small error in the location of the switching points can cause completely different motion behavior, we can still obtain a useful solution by minimizing the error with a

sufficiently small time step. The describing function technique based on the first approximation of Kryloff and Bogoliuboff gives reasonably accurate results for harmonic motion with one fundamental frequency. The method should not be used when a large harmonic is present. Extending the technique to higher harmonics is extremely complex and has not been attempted in nonlinear aeroelasticity. The point transformation method captures the switching points exactly, and the two formulations outlined in this paper are capable of predicting all types of airfoil motion, such as, stable, divergent, LCOs and chaotic motions.

References

[1] Lee, B.H.K., Price, S.J. and Wong, Y.S. Nonlinear aeroelastic analysis of airfoils: bifurcation and chaos. *Prog. in Aerosp. Sci.*, Vol. 35, No. 3, pp 205-334, 1999.

[2] Woolston, D.S., Runyan, H.L. and Andrews, R.E. An investigation of effects of certain types of structural nonlinearities on wing and control surface flutter. *J. Aeronaut. Sci.*, Vol. 24, No. 1, pp 57–63, 1957.

[3] Shen, S.F. An approximate analysis of nonlinear flutter problems. *J. Aerosp. Sci.*,Vol. 26, No. 1, pp 25–32, 1959.

[4] Lee, B.H.K., Jiang, L.Y. and Wong, Y.S. Flutter of an airfoil with a cubic restoring force. *J. Fluids Struct.*, Vol. 13, No. 1, pp 75-101, 1999.

[5] Liu, L. Wong, Y.S. and Lee, B.H.K. Application of the centre manifold theory in nonlinear aeroelasticity. *J. Sound Vib.*, Vol. 234, No. 4, pp 641-659, 2000.

[6] Liu, L. Wong, Y.S. and Lee, B.H.K. Nonlinear aeroelastic analysis using the point transformation method, part I: freeplay models. *J. Sound Vib.* (to be published).

[7] Fung, Y.C., *An introduction to the theory of aeroelasticity*. John Wiley and Sons, N.Y., 1955.

[8] Lee, B.H.K. and Desrochers, J. Flutter analysis of a two-dimensional airfoil containing structural nonlinearities. National Research Council Canada, LR-618, May, 1987.

[9] Jones, R.T. The unsteady lift of a wing of finite aspect ratio. *NACA Rept.* 681, 1940.

[10] Lee, B.H.K., Gong, L. and Wong, Y.S. Analysis and computation of nonlinear dynamic response of a two-degree-of-freedom system and its application in aeroelasticity. *J. Fluids Struct.*, Vol. 11, pp 225-246, 1997.

[11] Houbolt, J.C. A recurrence matrix solution for the dynamic response of elastic aircraft. *J. Aeronaut. Sci.*, Vol. 17, No. 9, pp 540-550, 1950.

[12] Jones, D.J. and Lee, B.H.K. Time marching numerical solution of the dynamic response of nonlinear systems. National Research Council Canada, NAE-AN-25, Jan. 1985.

[13] Bathe, K.J. and Wilson, E.L. *Numerical methods in finite element analysis*. Prentice-Hall Inc., Englewood Cliffs, N.J., 1976.

[14] Liu, L., Wong, Y.S. and Lee, B.H.K. Error analysis of Runge-Kutta's discretizations for certain types of systems. *J. Sound Vib.* (submitted).

[15] Kryloff, N. and Bogoliuboff, N. *Introduction to nonlinear mechanics.* Princeton University Press, Princeton, 1947.

[16] Price, S.J., Alighanbari, H. and Lee, B.H.K. The aeroelastic response of a two-dimensional airfoil with bilinear and cubic structural nonlinearities. *J. Fluids Struct.*, Vol. 9, pp 175-193, 1995.

[17] Johnson, E.C. Sinusoidal analysis of feedback-control systems containing nonlinear elements. *Trans. AIEE*, Vol. 71, pp 169-181, 1952.

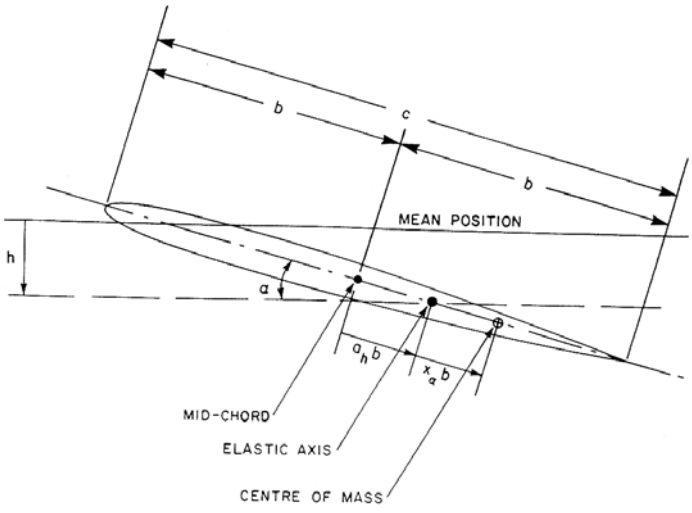

Fig. 1 Schematic of airfoil.

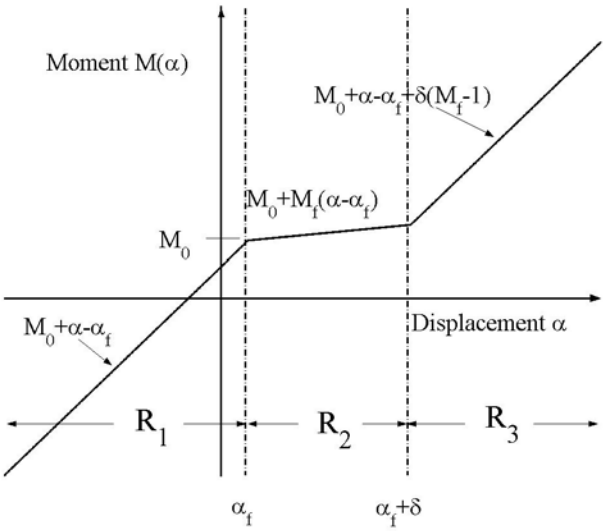

Fig. 2 Schematic of a freeplay.

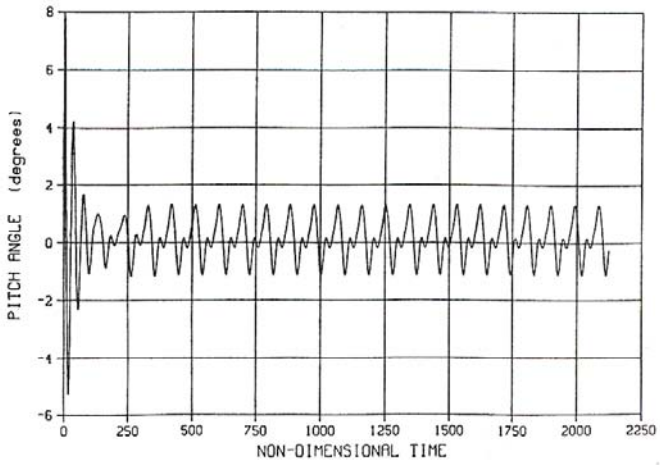

Fig. 4 Time variation of pitch angle from Houbolt's scheme for $U^*/U_L^* = 0.78$ and $\alpha(0) = 8^o$.

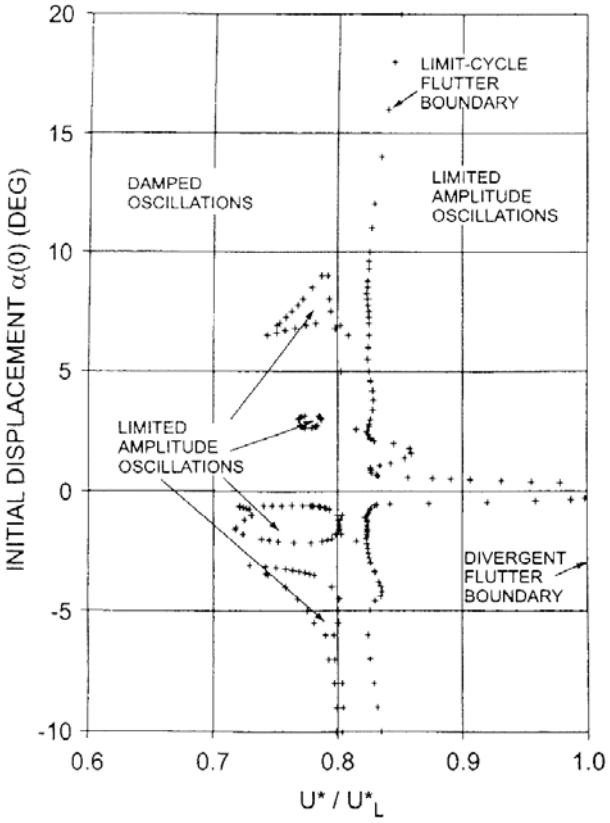

Fig. 3 Flutter boundary for $\overline{\omega} = 0.2$, $\mu = 100$, $\alpha_f = 0.25^o$, $\delta = 0.5^o$ and $M_0 = 0.25^o$.

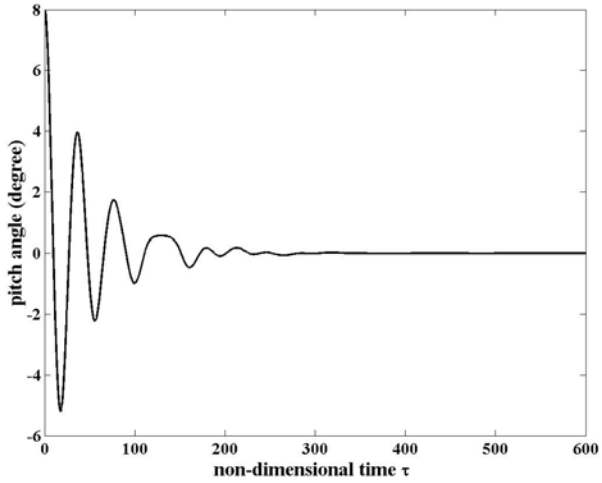

Fig. 5 Time variation of pitch angle from Runge- Kutta scheme for $U^*/U_L^* = 0.78$ and $\alpha(0) = 8^o$.

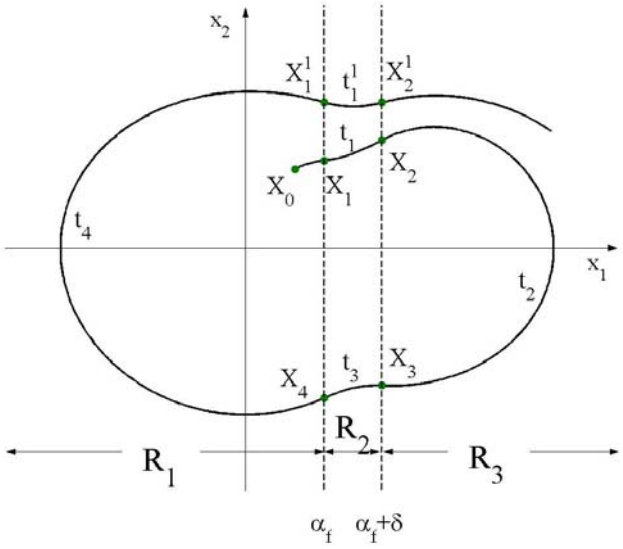

Fig. 6 Phase path of pitch angle from the point transformation method.

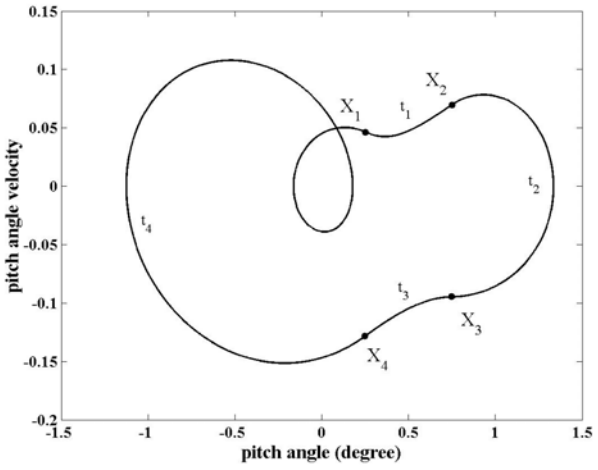

Fig. 7 Pitch velocity versus pitch angle for $U^*/U_L^* = 0.78$ and $\alpha(0) = 9^o$ from the point transformation method.

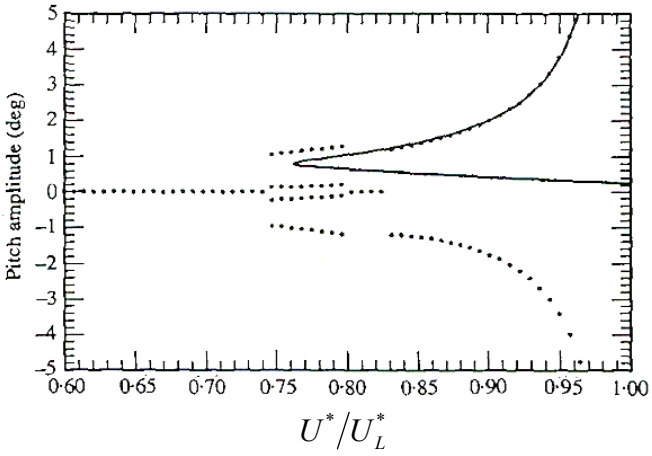

Fig. 8 Comparison of the limit cycle amplitude obtained from Houbolt's scheme and the describing function method.

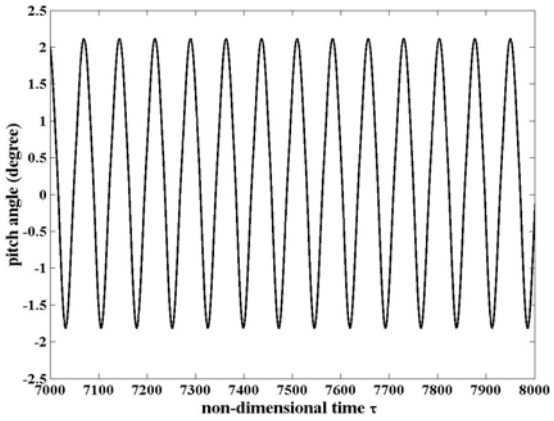

Fig. 9 Pitch angle versus time for $U^*/U_L^* = 0.9$ and $\alpha(0) = -1.0^o$ from the point transformation method.

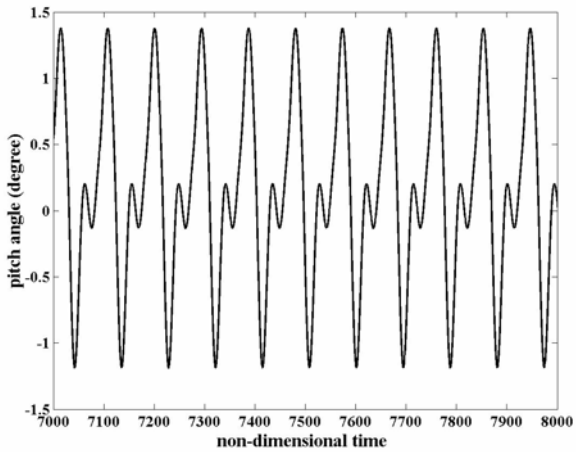

Fig. 10 Pitch angle versus time for $U^*/U_L^* = 0.79$ and $\alpha(0) = -1.0^o$ from the point transformation method.